Int J Clin Exp Med 2019;12(7):8662-8669
www.ijcem.com /ISSN:1940-5901/IJCEM0087952

Original Article

Identifying key genes in rheumatoid arthritis using bioinformatics analysis

Xing Song, Xiaofeng Zeng

Department of Rheumatology, Peking Union Medical College Hospital, Peking Union Medical College & Chinese Academy of Medical Sciences, Beijing, China

Received November 6, 2018; Accepted March 5, 2019; Epub July 15, 2019; Published July 30, 2019

Abstract: Rheumatoid arthritis (RA) is a common autoimmune disease. The aim of our study was to identify the key genes in RA using bioinformatics analysis. We downloaded the gene expression profiles of GSE17755 from the Gene Expression Omnibus (GEO) database and screened for differentially expressed genes (DEGs) using the limma package in R. The functional enrichment analysis of the DEGs was performed using DAVID. Selected DEGs were entered into STRING to construct a PPI network. Finally, subnetworks were visualized in Cytoscape to identify the hub genes. A total of 469 DEGs were identified, including 229 upregulated and 240 downregulated genes. A GO analysis showed that the upregulated genes were mainly enriched in the inflammatory response, but the downregulated genes were associated with cell-cell adhesion and translation. A KEGG pathway analysis showed that the downregulated genes were significantly enriched in antigen processing and presentation; conversely, upregulated genes were not significantly enriched in any KEGG pathway. The downregulated DEGs were entered into STRING, and two subnetworks were constructed. HSPA8 and RPL3 were identified as the most significant hub genes. HSPA8, RPL3 and their closely related genes and signaling pathways have potentially important roles in the onset and progression of RA. These genes may represent potential new targets for the treatment of RA.

Keywords: Bioinformatics, rheumatoid arthritis, key genes, HSPA8, RPL3

Introduction

Rheumatoid arthritis (RA) is a common chronic autoimmune disease with a worldwide incidence of approximately 1% [1]. RA involves multiple systems and is characterized by persistent inflammatory synovitis of the peripheral joints. Failure to control inflammation over time causes cartilage damage, bone erosion, and joint ankylosis, leading to joint deformity and loss of function [2]. The pathogenesis of RA remains unclear. Early diagnosis, disease and therapeutic monitoring, and prognostic evaluation have long been the focus of rheumatology research. With the progress in molecular biological technology, knowledge of the molecular and cellular processes involved in disease pathology mechanisms has increased, and gene microarray technology has recently been used for diagnosis and treatment [3]. Therefore, gene microarray research has also become popular in the RA field.

Joint inflammation in RA is mainly caused by different cells of the synovium and cartilage and gene products produced by infiltrating cells from the circulation. Therefore, the study of RA mainly involves joint synovial tissue and peripheral blood, and the application of gene microarray technology enables us to better understand the role of joint synovial tissue and peripheral blood in RA. In a previous literature review, we found that differential gene analysis of RA typically involves the microarray analysis of synovial cells to compare RA and healthy controls, RA and osteoarthritis (OA), or RA, OA, and HC to identify the differentially expressed genes (DEGs) [4, 5]. RA is a systemic autoimmune disease, and blood cells enter diseased tissue from the circulatory system and cause inflammatory cell infiltration as well as other pathological processes. Accordingly, the study of gene expression profiles in the peripheral blood is of great significance. In addition, the use of peripheral blood is convenient for research purposes, as it is suitable for evaluating genetic

susceptibility in a large cohort. The purpose of this study was to identify key genes in RA by analyzing the gene expression profiles.

Methods

Data collection

The NCBI Gene Expression Omnibus (GEO) database provides a large collection of microarray expression data [6]. "Rheumatoid Arthritis" was used as the keyword to search for RA expression profiling. mRNA expression profiling datasets were included based on the following criteria: (1) the dataset was generated from the peripheral blood cells of patients with RA; (2) the expression profiles of the peripheral blood cells of RA patients and healthy in dividuals were available in the dataset; and (3) the RA patients had no treatment record before the peripheral blood cell collection. The GSE17755, GSE15573, GSE68689, and GSE100191 datasets were selected. There were 112 patients with RA and 45 healthy individuals in the GSE17755 dataset, which had the largest sample size among the selected studies.

Therefore, the GSE17755 series was selected for this research; these microarray data were obtained using a GPL1291 platform and submitted by Lee and colleagues [7]. A total of 244 samples comprise this series, including 112 RA and 45 healthy control samples. Thus, a total of 157 samples from this dataset were selected in the present study for subsequent analysis. Ethics approval was not required because we downloaded the expression profiles from a public database and did not perform any experiments on patients or animals.

Data preprocessing

We downloaded the GSE17755 series matrix file, and the probe names for the GPL1291 platform were transformed into gene symbols based on the Hitachisoft AceGene Human Chip 30K Chip Version 1. If multiple probes corresponded to the same gene symbol, the mean value was calculated using the aggregate function in R as the expression value of that particular gene. If the expression value of the probe was absent, the nearest neighbor average (KNN) algorithm in the impute package of R was used [8]. The obtained data were standardized.

DEG analysis

The DEGs in the RA samples compared with the healthy controls were screened using the *t* test in the limma package of R [9]. Then, the *P* value was adjusted using the FDR method. Only those genes with a fold change greater than 1.5 and an adjusted *P* value < 0.05 were recognized as significantly differentially expressed. The DEGs were classified as upregulated or downregulated according to the fold changes in their expressions. We generated a volcano map and a heat map of the DEGs using the R package.

Functional enrichment analysis of DEGs

We utilized the online tool DAVID (Database for Annotation Visualization and Integrated Discovery, National Institute of Allergy and Infectious Disease) to identify Gene Ontology (GO) categories and KEGG pathways [10]. Upregulated and downregulated genes were submitted to DAVID. Significantly enriched results were identified at $P < 0.05$.

Construction of a protein-protein interaction (PPI) network and identification of hub genes

We entered the DEGs into STRING (the Search Tool for the Retrieval of Interacting Genes) to construct a PPI network to evaluate the relationships among genes. A confidence score > 0.9 was defined as significant [11]. A cluster analysis was utilized to construct subnetworks of the obtained PPI network. We used the analysis function in STRING to enrich for the genes related to the Biological Processes and KEGG pathways. Then, subnetworks were visualized using Cytoscape software, a tool for the generation of integrated models of biologic molecular interaction networks. Twelve algorithms in the Cytoscape plugin cytoHubba were used to identify the hub genes in the subnetworks [12].

Results

DEG analysis

According to the above methods, we obtained 469 DEGs in the RA samples compared with the healthy controls, including 229 upregulated genes and 240 downregulated genes (**Figure 1A**). According to the descending order of the adjusted *P* value, the top 20 upregulated and downregulated genes were selected to generate a heatmap by cluster analysis (**Figure 1B**).

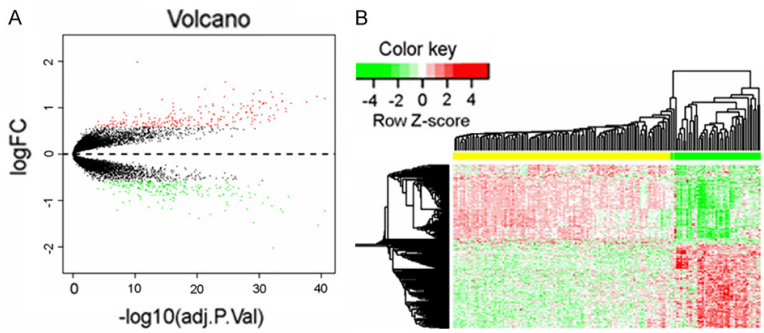

Figure 1. A. Volcano map of DEGs. Red points represent upregulated genes, green points represent downregulated genes, and black points represent non-DEGs in the microarray. B. Heat map of DEGs. The horizontal ordinate represents each sample, and the vertical ordinate corresponds to each gene. The yellow bar represents RA samples, and the green bar represents healthy control samples.

Functional enrichment analysis of DEGs

The upregulated and downregulated genes were submitted to DAVID for gene function enrichment analysis to identify the most significant GO categories and KEGG pathways. We sorted the enrichment results in descending order by adjusted *P* value, with-LOG10 (*P* value) on the X-axis. The top 10 results are shown in **Figure 2**.

The GO analysis showed that upregulated genes were significantly associated with the defense response to a bacterium, an inflammatory response, and the positive regulation of catalytic activity in the Biological Process (BP) category; integral component of the membrane, integral component of the plasma membrane, and synapse in the Cellular Component (CC) category; and RAGE receptor binding, transcriptional activator activity, and epidermal growth factor receptor binding in the Molecular Function (MF) category. Downregulated genes were mainly enriched in cell-cell adhesion, translation, and cellular response to interleukin-4 in the BP category; extracellular exosome, membrane, and focal adhesion in the CC category; and protein binding, poly(A) RNA binding, and cadherin binding involved in cell-cell adhesion in the MF category. **Figure 2** shows more than 10 enrichment results in all three GO categories for the downregulated genes; only 4 results in CC and MF were found for the upregulated genes.

Similarly, our KEGG pathway analysis showed that downregulated genes were significantly enriched in antigen processing and presentation, platelet activation, and HTLV-I infection, with RA ranking sixth (**Figure 2G**). Strikingly, the upregulated genes showed no significant enrichment in the KEGG pathway analysis.

Construction of the PPI network and identification of hub genes

A total of 240 downregulated genes were submitted to the online tool STRING for the construction of a PPI network, which consisted of 235 nodes and 354 edges. Two subnetworks were indicated by a cluster analysis (**Figure 3**). One subnetwork (green) consisted of 26 nodes and 152 edges, with marked functional enrichment in mRNA splicing in the BP GO term as well as the spliceosome pathway in the KEGG pathway analysis (**Table 1**). The other subnetwork (dark cyan) included 15 nodes and 63 edges, with functional enrichment in translation in the BP GO term and the Ribosome pathway in the KEGG pathway analysis (**Table 2**).

Two subnetworks were visualized using Cytoscape software, and we applied the Cytoscape plugin cytoHubba to identify the hub genes. This comprehensive evaluation identified the most significant hub gene as HSPA8 in the green subnetwork (degree = 25, closeness = 25, and radiality = 2.12); other hub genes included HNRNPA1, SRSF5, SNRNP70, and SMNDC1. In the dark cyan subnetwork, the most significant hub gene was RPL3 (degree = 14, closeness = 14, and radiality = 2.21); other hub genes included RPL29, RPL8, SRPR, and EIF3D (**Figure 4A**, **4B**, Tables S1, S2).

Discussion

RA is a systemic immune disorder of complex etiology that is related to interactions among various cells and cytokines. Gene microarrays have identified the roles of the genes, cells and cytokines in the pathogenesis of RA. At present, the bioinformatics analysis of RA has primarily focused on synovial tissues. In our study, however, gene expression in peripheral blood examined selected, a more suitable choice for RA as a disease involving multiple systems.

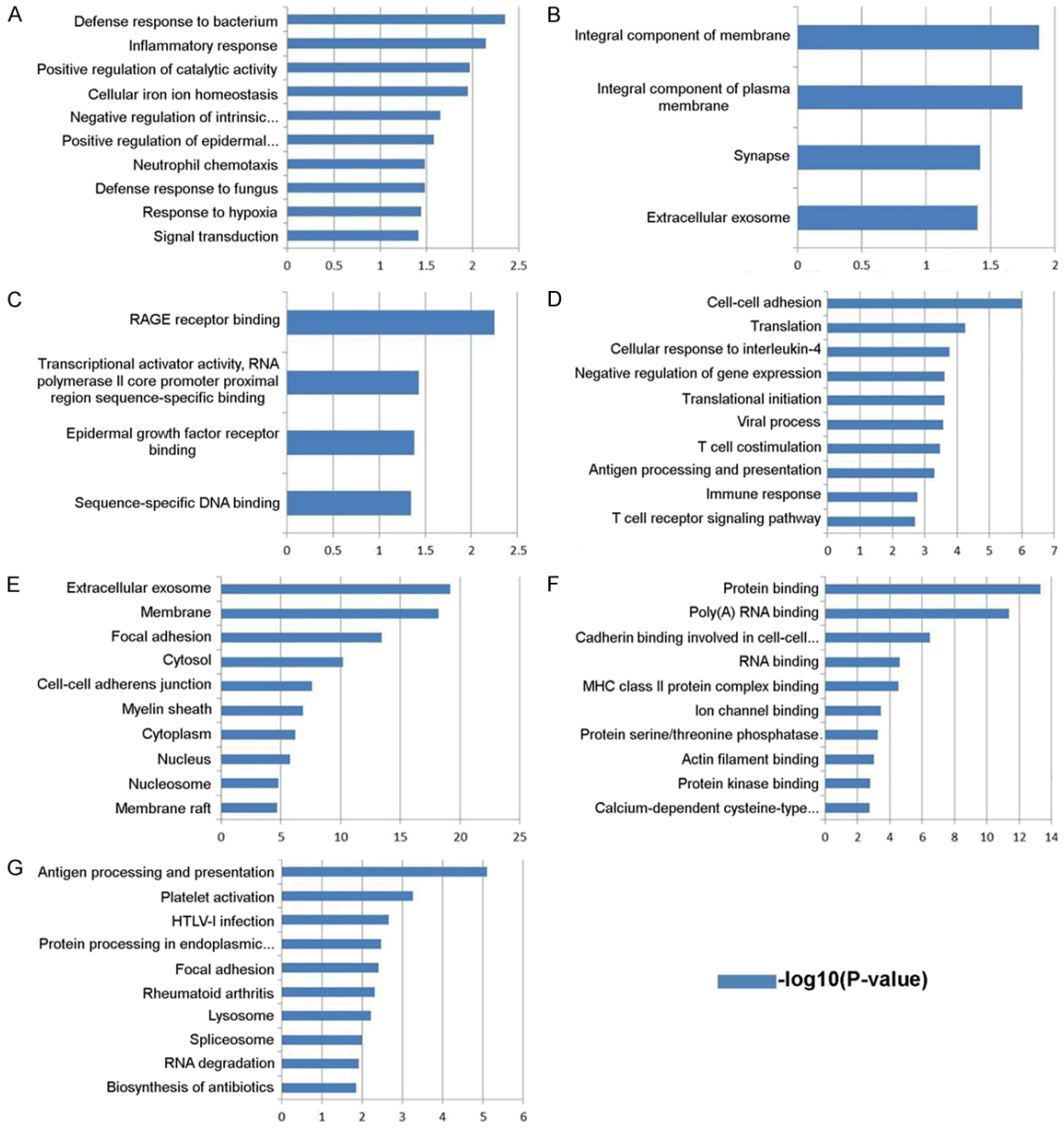

Figure 2. A-C. Upregulated genes enriched in the BP, CC, and MF GO terms. D-F. Downregulated genes enriched in the BP, CC, and MF GO terms. G. Downregulated genes enriched in KEGG pathways. BP, Biological Process; CC, Cellular Component; MF, Molecular Function; GO, Gene Ontology.

GSE17755 is currently the largest RA gene expression dataset in the GEO database. We extracted data from GSE17755 and identified 469 DEGs between the RA samples and healthy controls, including 229 upregulated genes and 240 downregulated genes. An enrichment analysis revealed that the downregulated genes were mainly enriched in cell-cell adhesion, translation, and antigen processing and presentation pathways. Most importantly, we found strong enrichment in a very small number of GO terms and no significant enrichment in KEGG pathways for upregulated genes. Therefore, we speculated that downregulated genes play a more important role in RA than do upregulated genes. This hypothesis is similar to that proposed in a previous study by Hao [13].

Next, we entered the 240 downregulated genes into the online tool STRING to build the PPI network. Cluster analysis revealed two subnetworks. Generally, subnetworks are clusters of

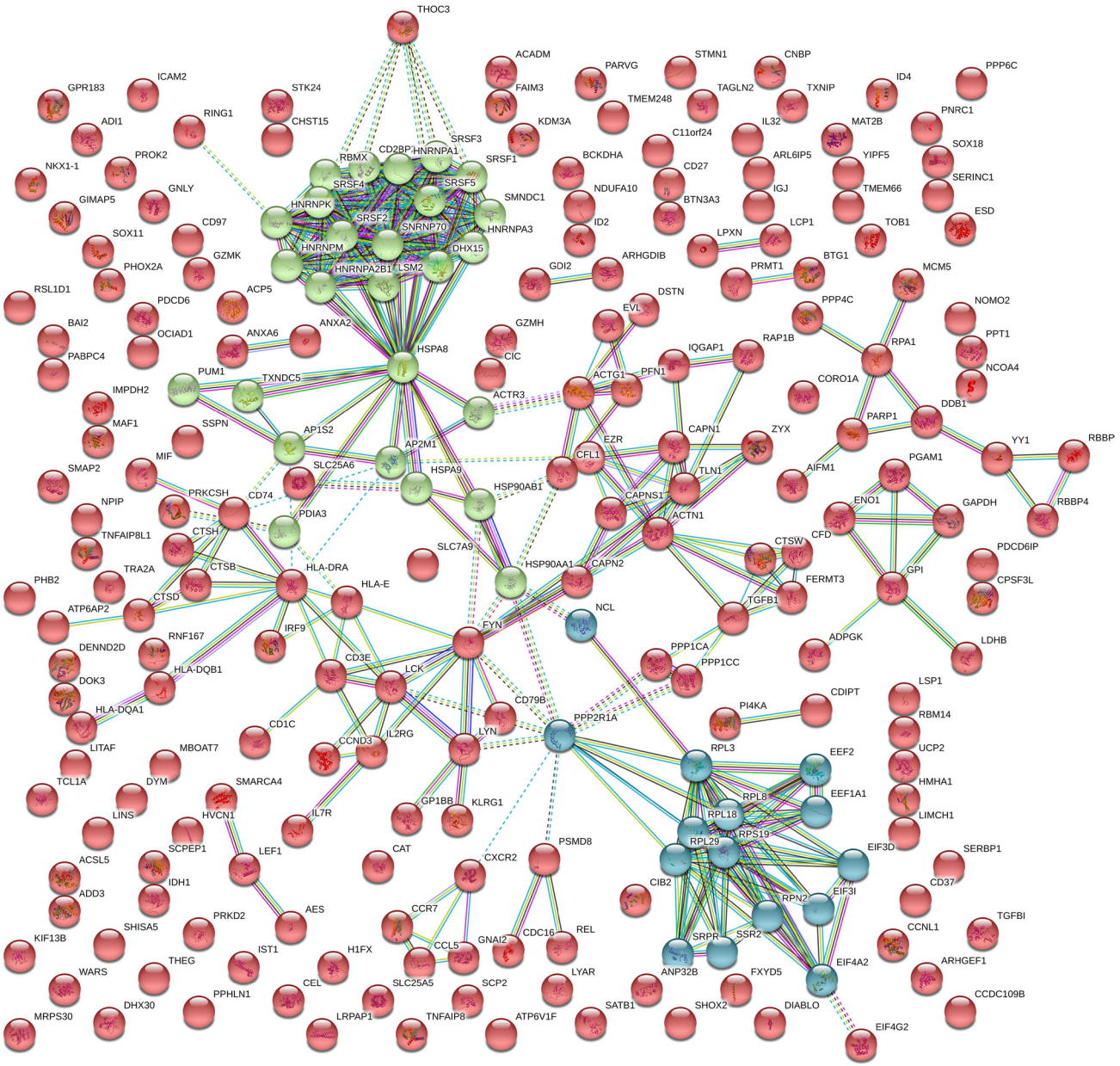

Figure 3. The downregulated genes were submitted to the online tool STRING for construction of the PPI network. The green and dark cyan nodes represent two subnetworks.

Table 1. GO and KEGG pathway analysis of genes in the first subnetwork (green)

Biological Process (GO)			
Pathway ID	*Pathway description*	*Count in gene set*	*False discovery rate*
GO:0000398	mRNA splicing, via spliceosome	13	4.38e-16
GO:0008380	RNA splicing	14	1.21e-15
GO:0006397	mRNA processing	14	1.12e-14
GO:0048024	regulation of mRNA splicing, via spliceosome	7	6.5e-10
GO:0050658	RNA transport	8	9.75e-09
KEGG Pathways			
Pathway ID	*Pathway description*	*Count in gene set*	*False discovery rate*
03040	spliceosome	14	1.11e-22
05168	Herpes simplex infection	6	9.96e-06
04141	protein processing in endoplasmic reticulum	5	0.000121
04612	antigen processing and presentation	4	0.000121
04915	estrogen signaling pathway	3	0.0126

Table 2. GO and KEGG pathway analysis of genes in the second subnetwork (dark cyan)

Biological Process (GO)			
Pathway ID	*Pathway description*	*Count in gene set*	*False discovery rate*
GO:0006412	translation	11	2.3e-13
GO:0043603	cellular amide metabolic process	12	3.41e-13
GO:0006614	SRP-dependent cotranslational protein targeting to membrane	8	5.8e-12
GO:1901564	organonitrogen compound metabolic process	12	6.38e-09
GO:0000956	nuclear-transcribed mRNA catabolic process	7	1.41e-08
KEGG Pathways			
Pathway ID	*Pathway description*	*Count in gene set*	*False discovery rate*
03010	ribosome	5	7.27e-06
03013	RNA transport	4	0.000524

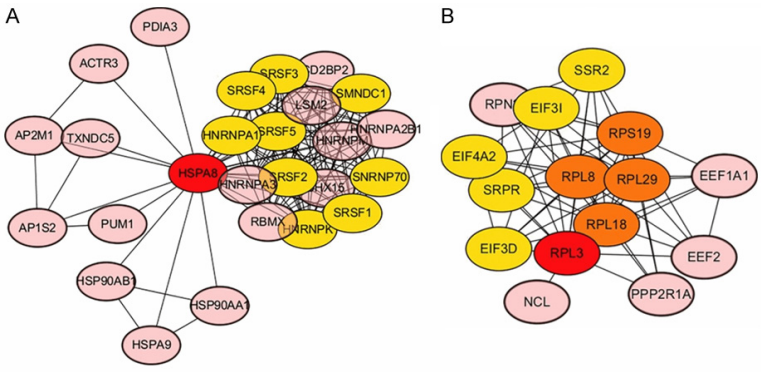

Figure 4. The subnetworks were visualized by Cytoscape software. CytoHubba was used to identify the hub genes. (A) Green subnetwork, (B) Dark cyan subnetwork. Different colors indicate different degrees of importance, decreasing from red to orange, yellow and pink.

related genes that have a similar biological function [14]. The first subnetwork mainly involved RNA splicing, and the gene connections were very close. The other subnetwork primarily involved translation and RNA transport. Therefore, we speculated that RNA regulation plays a key role in the pathogenesis of RA.

Further analysis of the subnetworks by cytoHubba revealed HSPA8 as the most important hub gene in the first subnetwork. HSPA8, a chaperone protein, interacts with various other gene products, such as HNRNPA1, SRSF5, SNRNP70, and SMNDC1, and is a cognate protein of the Hsp70 family, which is central to many cellular processes [15]. Its functions contribute to numerous biological processes, including signal transduction, apoptosis, autophagy, protein homeostasis, and cell growth and differentiation [16], and HSPA8 has been associated with an extensive number of cancers and neurode-

generative diseases, as well as cell senescence and aging [17, 18]. In particular, Hsp70 family members play a protective role in many diseases. The protective role of HSPA8 was further highlighted in a study that identified it alongside other HSP70 proteins in a core subnetwork of the wider chaperone interactome that functions as a proteostasis safeguard and that is repressed in aging brains and in the brains of patients with Alzheimer's, Parkinson's or Huntington's disease [19].

There is ample evidence that Hsp70 contributes to the progression of RA [20-22]. These data imply that genetic variants of Hsp70 genes, such as the HSPA8 gene, might contribute to the development of RA. At present, studies on HSPA8 in RA are limited. One research article reported that HSPA8 is related to fatty acid metabolism, and the IκB kinase/NF-κB cascade is a significant biomarker of the traditional Chinese medicine heat pattern of RA [23]. However, this study was a bioinformatics analysis that has not been confirmed by appropriate experiments. We have reason to support the correlation between HSPA8 downregulation and regulatory T and B cells, TNF-α, IL-6, IL-10 and other cells and cytokines closely related to RA pathogenesis.

RPL3, a hub gene in the other subnetwork, plays an important biological role through interactions with proteins such as RPL29, RPL8, SRPR, and EIF3D. RPL3 is a component of the large subunit of cytoplasmic ribosomes, which is associated with many cancers. Russo and colleagues found that RPL3 downregulation correlated positively with multidrug resistance in cancer [24]. The mechanism may be related to the control of cell redox status, and upregulating RPL3 is a potential therapeutic approach for treating p53-negative cancers [25]. At present, PubMed does not contain any reports on RPL3 in RA. Thus, further studies on RPL3 may help explain the pathogenesis of RA and guide targeted therapy.

As mentioned above, our research remains in the bioinformatics analysis stage, and our observations and hypotheses must be verified through a large number of appropriate experiments, such as quantitative real-time PCR and western blot analysis.

Conclusion

Our study showed that downregulated genes play an important role in RA and that HSPA8 and its related genes and signaling pathways are key in the progression and development of RA. Future studies on these genes are likely to confirm our conclusions, and these genes may become new targets for the treatment of RA.

Disclosure of conflict of interest

None.

Address correspondence to: Dr. Xiaofeng Zeng, Department of Rheumatology, Peking Union Medical College Hospital, No. 1 Shuaifuyuan, Dongcheng District, Beijing 100730, China. E-mail: zengxfpumc@foxmail.com

References

[1] Abhishek A, Doherty M, Kuo CF, Mallen CD, Zhang W and Grainge MJ. Rheumatoid arthritis is getting less frequent-results of a nationwide population-based cohort study. Rheumatology (Oxford) 2017; 56: 736-744.

[2] Gay S, Gay RE and Koopman WJ. Molecular and cellular mechanisms of joint destruction in rheumatoid arthritis: two cellular mechanisms explain joint destruction? Ann Rheum Dis 1993; 52: S39-47.

[3] Yoo SM, Choi JH, Lee SY and Yoo NC. Applications of DNA microarray in disease diagnostics. J Microbiol Biotechnol 2009; 19: 635-46.

[4] Liu T, Lin X and Yu H. Identifying genes related with rheumatoid arthritis via system biology analysis. Gene 2015; 571: 97-106.

[5] Gang X, Sun Y, Li F, Yu T, Jiang Z, Zhu X, Jiang Q and Wang Y. Identification of key genes associated with rheumatoid arthritis with bioinformatics approach. Medicine (Baltimore) 2017; 96: e7673.

[6] Edgar R, Domrachev M, Lash AE. Gene expression omnibus: NCBI gene expression and hybridization array data repository. Nucleic Acids Res 2002; 30: 207-10.

[7] Lee HM, Sugino H, Aoki C and Nishimoto N. Underexpression of mitochondrial-DNA encoded ATP synthesis-related genes and DNA repair genes in systemic lupus erythematosus. Arthritis Res Ther 2011; 13: R63.

[8] Altman NS. An introduction to kernel and nearest-neighbor nonparametric regression. Am Stat 1992; 46: 175-185.

[9] Smyth GK. limma: linear models for microarray data. Bioinformatics & Computational Biology Solutions Using R & Bioconductor 2011; 397-420.

[10] Huang DW, Sherman BT, Tan Q, Collins JR, Alvord WG, Roayaei J, Stephens R, Baseler MW, Lane HC and Lempicki RA. The DAVID gene functional classification tool: a novel biological module-centric algorithm to functionally ana-

lyze large gene lists. Genome Biol 2007; 8: R183.
[11] von Mering C, Huynen M, Jaeggi D, Schmidt S, Bork P and Snel B. STRING: a database of predicted functional associations between proteins. Nucleic Acids Res 2003; 31: 258-61.
[12] Chin CH, Chen SH, Wu HH, Ho CW, Ko MT and Lin CY. CytoHubba: identifying hub objects and sub-networks from complex interactome. BMC Syst Biol 2014; 8: S11.
[13] Hao R, Du H, Guo L, Tian F, An N, Yang T, Wang C, Wang B, Zhou Z. Identification of dysregulated genes in rheumatoid arthritis based on bioinformatics analysis. PeerJ 2017; 5: e3078.
[14] Ideker T, Ozier O, Schwikowski B and Siegel AF. Discovering regulatory and signalling circuits in molecular interaction networks. Bioinformatics 2002; 18: S233-40.
[15] Stricher F, Macri C, Ruff M and Muller S. HSPA8/HSC70 chaperone protein: structure, function, and chemical targeting. Autophagy 2013; 9: 1937-1954.
[16] Mayer MP and Bukau B. Hsp70 chaperones: cellular functions and molecular mechanism. Cell Mol Life Sci 2005; 62: 670-684.
[17] Wang X, Wang Q, Lin H, Li S, Sun L and Yang Y. HSP72 and gp96 in gastroenterological cancers. Clin Chim Acta 2013; 417: 73-79.
[18] Xilouri M and Stefanis L. Chaperone mediated autophagy in aging: starve to prosper. Ageing Res Rev 2016; 32: 13-21.
[19] Brehme M, Voisine C, Rolland T, Wachi S, Soper JH, Zhu Y, Kai O, Villella A, Dan G and Vidal M. A chaperome sub-network safeguards proteostasis in aging and neurodegenerative disease. Cell Rep 2014; 9: 1135-1150.
[20] Schett G, Redlich K, Xu Q, Bizan P, Gröger M, Tohidast-Akrad M, Kiener H, Smolen J, Steiner G. Enhanced expression of heat shock protein 70 (hsp70) and heat shock factor 1 (HSF1) activation in rheumatoid arthritis synovial tissue. Differential regulation of hsp70 expression and hsf1 activation in synovial fibroblasts by proinflammatory cytokines, shear stress, and antiinflammatory drugs. J Clin Invest 1998; 102: 302-11.
[21] Schick C, Arbogast M, Lowka K, Rzepka R, Melchers I. Continuous enhanced expression of Hsc70 but not Hsp70 in rheumatoid arthritis synovial tissue. Arthritis Rheum 2004; 50: 88-93.
[22] Moshrif A and Moshrif A. Diagnostic and prognostic values of serum HSP70 and YKL-40 in patients with rheumatoid arthritis. International Journal of Clinical Rheumatology 2017; 12: 59-66.
[23] Lu C, Niu X, Xiao C, Chen G, Zha Q, Guo H, Jiang M and Lu A. Network-based gene expression biomarkers for cold and heat patterns of rheumatoid arthritis in traditional Chinese medicine. Evid-Based Compl Alt 2012; 2012: 1-17.
[24] Russo A, Saide A, Smaldone S, Faraonio R and Russo G. Role of uL3 in multidrug resistance in p53-mutated lung cancer cells. Int J Mol Sci 2017; 18: 547.
[25] Pagliara V, Saide A, Mitidieri E, d'Emmanuele di Villa Bianca R, Sorrentino R, Russo G, Russo A. 5-FU targets rpL3 to induce mitochondrial apoptosis via cystathionine-β-synthase in colon cancer cells lacking p53. Oncotarget 2016; 7: 50333-50348.

Table S1. Twelve algorithms in cytoHubba revealed a green subnetwor

node_name	MCC	DMNC	MNC	Degree	EPC	BottleNeck	EcCentricity	Closeness	Radiality	Betweenness	Stress	Clustering Coefficient
HSPA8	2.09E + 13	1.0769	16	25	6.98	26	1	25	2.12	342	346	0.42333
PDIA3	1	0	1	1	1.475	1	0.5	13	1.16	0	0	0
PUM1	2	0.30779	2	2	1.663	1	0.5	13.5	1.2	0	0	1
ACTR3	2	0.30779	2	2	1.742	1	0.5	13.5	1.2	0	0	1
CD2BP2	2.09E + 13	1.0769	16	16	6.26	1	0.5	20.5	1.76	0	0	1
AP1S2	6	0.2842	4	4	1.854	1	0.5	14.5	1.28	3	6	0.5
AP2M1	4	0.30898	3	3	1.802	1	0.5	14	1.24	1	2	0.66667
TXNDC5	2	0.30779	2	2	1.712	1	0.5	13.5	1.2	0	0	1
SMNDC1	2.09E + 13	1.0769	16	16	6.367	1	0.5	20.5	1.76	0	0	1
HSPA9	6	0.46346	3	3	1.845	1	0.5	14	1.24	0	0	1
RBMX	2.09E + 13	1.0769	16	16	6.471	1	0.5	20.5	1.76	0	0	1
HNRNPA2B1	2.09E + 13	1.0769	16	16	6.374	1	0.5	20.5	1.76	0	0	1
HNRNPA3	2.09E + 13	1.0769	16	16	6.34	1	0.5	20.5	1.76	0	0	1
HNRNPM	2.09E + 13	1.0769	16	16	6.411	1	0.5	20.5	1.76	0	0	1
LSM2	2.09E + 13	1.0769	16	16	6.35	1	0.5	20.5	1.76	0	0	1
DHX15	2.09E + 13	1.0769	16	16	6.388	1	0.5	20.5	1.76	0	0	1
SRSF5	2.09E + 13	1.0769	16	16	6.222	1	0.5	20.5	1.76	0	0	1
HNRNPA1	2.09E + 13	1.0769	16	16	6.078	1	0.5	20.5	1.76	0	0	1
HNRNPK	2.09E + 13	1.0769	16	16	6.485	1	0.5	20.5	1.76	0	0	1
SNRNP70	2.09E + 13	1.0769	16	16	6.449	1	0.5	20.5	1.76	0	0	1
SRSF4	2.09E + 13	1.0769	16	16	6.236	1	0.5	20.5	1.76	0	0	1
SRSF3	2.09E + 13	1.0769	16	16	6.584	1	0.5	20.5	1.76	0	0	1
HSP90AB1	6	0.46346	3	3	1.951	1	0.5	14	1.24	0	0	1
HSP90AA1	6	0.46346	3	3	1.792	1	0.5	14	1.24	0	0	1
SRSF1	2.09E + 13	1.0769	16	16	6.373	1	0.5	20.5	1.76	0	0	1
SRSF2	2.09E + 13	1.0769	16	16	6.506	1	0.5	20.5	1.76	0	0	1

Table S2. Twelve algorithms in cytoHubba revealed a dark cyan subnetwork

node_name	MCC	DMNC	MNC	Degree	EPC	BottleNeck	EcCentricity	Closeness	Radiality	Betweenness	Stress	Clustering Coefficient
RPL3	10921	0.62588	13	14	8.106	2	1	14	2.21429	37.6	84	0.53846
PPP2R1A	120	0.64826	5	5	5.709	1	0.5	9.5	1.57143	0	0	1
RPN2	5040	0.76834	7	7	6.724	1	0.5	10.5	1.71429	0	0	1
SSR2	5040	0.76834	7	7	6.609	1	0.5	10.5	1.71429	0	0	1
NCL	1	0	1	1	2.338	1	0.5	7.5	1.28571	0	0	0
EIF4A2	5040	0.76834	7	7	6.61	1	0.5	10.5	1.71429	0	0	1
SRPR	5040	0.76834	7	7	6.664	1	0.5	10.5	1.71429	0	0	1
RPL29	10920	0.62588	13	13	8.048	10	0.5	13.5	2.14286	11.6	58	0.62821
EEF1A1	720	0.71324	6	6	6.45	1	0.5	10	1.64286	0	0	1
EIF3D	5040	0.76834	7	7	6.699	1	0.5	10.5	1.71429	0	0	1
EIF3I	5040	0.76834	7	7	6.699	1	0.5	10.5	1.71429	0	0	1
EEF2	720	0.71324	6	6	6.205	1	0.5	10	1.64286	0	0	1
RPL8	10920	0.62588	13	13	8.124	1	0.5	13.5	2.14286	11.6	58	0.62821
RPL18	10920	0.62588	13	13	8.116	1	0.5	13.5	2.14286	11.6	58	0.62821
RPS19	10920	0.62588	13	13	8.159	1	0.5	13.5	2.14286	11.6	58	0.62821